

viate strongly from the $J(J+1)$ spacing expected for a pure band, suggesting appreciable mixing. A band-mixing calculation⁸ has shown that the ground-state band contains large ($\sim 10\%$ in intensity) admixtures from three orbitals besides the $\frac{3}{2}^+$ [211] orbital; namely the $\frac{1}{2}^+$ [211], $\frac{5}{2}^+$ [202], and $\frac{1}{2}^+$ [220] orbitals. A similar calculation using the above four positive-parity bands resulted in the relative reduced $E1$ strengths shown in Table I. The deformation was fixed at $\delta=0.32$ for all bands and the band-head energies and moment-of-inertia parameters ($\hbar^2/2I$) were varied to give reasonable energy-level fits. Although the agreement with experiment is not complete, the results appear to exhibit the correct trend and do not critically depend on the choice of parameters. Band mixing thus appears to account for the gross features of the above-mentioned general behavior of the $E1$ rates. It can be shown that this behavior results primarily from the presence of the admixed $\frac{1}{2}^+$ [211] wave function while the $J(J+1)$ energy deviation results mainly from

the addition of the strongly decoupled $\frac{1}{2}^+$ [220] band.

[†]Work supported by a grant from the National Research Council of Canada.

¹J. A. Kuehner and E. Almqvist, *Can. J. Phys.* **45**, 1605 (1967).

²E. R. Cosman, A. Sperduto, W. H. Moore, T. N. Chan, and T. M. Cormier, *Phys. Rev. Lett.* **27**, 1074 (1971).

³A. E. Blaugrund, *Nucl. Phys.* **88**, 501 (1966).

⁴L. C. Northcliffe and R. F. Schilling, *Nucl. Data, Sect. A* **7**, 233 (1970).

⁵J. L. Durell, P. R. Alderson, D. C. Bailey, L. L. Greene, A. N. James, and J. F. Sharpey-Shafer, *Phys. Lett.* **29B**, 100 (1969).

⁶R. A. Lindgren, J. G. Pronko, R. G. Hirko, D. A. Bromley, and J. W. Olness, *Bull. Amer. Phys. Soc.* **14**, 531 (1969), and private communication.

⁷G. Alaga, K. Alder, A. Bohr, and B. R. Mottleson, *Kgl. Dan. Vidensk. Selsk., Mat.-Fys. Medd.* **29**, No. 9 (1955).

⁸J. Dubois, *Nucl. Phys.* **A104**, 657 (1967).

SU(3) Comparison of φ and $K(890)$ Production*

M. Aguilar-Benitez, S. U. Chung, R. L. Eisner, and N. P. Samios

Brookhaven National Laboratory, Upton, New York 11973

(Received 17 December 1971)

We have utilized SU(3) invariance to relate the reactions $K^-p \rightarrow (\Lambda, \Sigma^0)\varphi$ with $\pi^-p \rightarrow (\Lambda, \Sigma^0)K(890)$ in the peripheral region. We find that in all observable distributions, including the baryon polarization and the vector-meson density-matrix elements, the data are in good agreement with the SU(3) predictions. These observations lead us to conclude that potential sources for the symmetry breaking, such as external-mass-dependent factors or absorptive effects, do not significantly affect the simple SU(3) picture.

The SU(3) symmetry scheme has been remarkably successful in describing the spectroscopy of the well-known boson and baryon states. The situation with regard to dynamics (i.e., predicting relations among cross sections) has been less clear.¹ In this Letter we address ourselves to several SU(3) dynamical predictions which satisfy the expected regularities to within the experimental errors. These involve reactions (whose relationship is not entirely transparent) in which vector mesons are produced via a meson exchange process with the baryon vertex remaining invariant. The most noteworthy previous such example has been the similarity of ω and ρ^0 production and decay characteristics as measured in K^-p interactions.² Here we examine differential

cross sections, polarization, and density-matrix elements of $\varphi(1020)$ and $K(890)$ produced in the following channels:

$$K^-p \rightarrow \Lambda\varphi, \quad (1a)$$

$$\rightarrow \Sigma^0\varphi, \quad (1b)$$

$$\pi^-p \rightarrow \Lambda K(890), \quad (2a)$$

$$\rightarrow \Sigma^0 K(890). \quad (2b)$$

If the production mechanism of Reactions (1) and (2) is meson exchange, they can be related to each other by application of SU(3) symmetry at the meson vertex, since the baryon vertex remains the same. Very little needs to be assumed about the nature of the exchanged meson. If K

or $K(1420)$ is exchanged in the process, the meson vertex requires the antisymmetric F type of coupling, whereas if the $K(890)$ is responsible for the exchange mechanism, the meson vertex involves the symmetric D -type coupling. In either case, the $SU(3)$ symmetry leads to the following relation for each helicity amplitude³:

$$A(K^-p \rightarrow Y\varphi) = -A(\pi^-p \rightarrow YK(890)), \quad (3)$$

where we have suppressed the helicity indices and Y stands for either Λ or Σ^0 . In this derivation we have used the experimentally observed small value of the $\varphi \rightarrow \rho\pi$ branching ratio as well as the ideal mixing angle between the ω and φ (35° which is essentially equal to the experimental value of $\sim 39^\circ$). We have in addition assumed that neither the factors in the amplitude which depend on the external masses nor absorptive effects strongly break this equality (3).

This in turn leads to the following relationships among the experimentally measured quantities as examined in the peripheral region:

$$\frac{d\sigma}{dt}(K^-p \rightarrow Y\varphi) = \frac{d\sigma}{dt}(\pi^-p \rightarrow YK(890)), \quad (4)$$

$$P_Y(K^-p \rightarrow Y\varphi) = P_Y(\pi^-p \rightarrow YK(890)), \quad (5)$$

$$\rho_{mm'}(K^-p \rightarrow Y\varphi) = \rho_{mm'}(\pi^-p \rightarrow YK(890)), \quad (6)$$

with $\bar{\sigma} \equiv \sum |A|^2 = (P_{\text{in}}/P_{\text{out}})S\sigma$, S being the square of the center-of-mass energy.⁴ P_Y and $\rho_{mm'}$ are the baryon polarization and vector-meson density-matrix elements, respectively.

We now turn to a comparison of relations (4)–(6) with the experimental data. The study of K^-p interactions comes from exposures of the Brookhaven National Laboratory 80-in. hydrogen-filled bubble chamber to beams of K^- mesons at 3.9 and 4.6 GeV/ c incident momenta. The reactions of interest⁵ are

$$K^-p \rightarrow \Lambda K^+K^-, \quad (7)$$

$$\rightarrow \Lambda K_1^0(K^0), \quad (8)$$

$$\rightarrow \Sigma^0 K^+K^-, \quad (9)$$

where the symbol (K^0) represents an unseen K^0 decay. The event separation between the Λ and Σ^0 hypotheses is described in another publication.⁶ We merely note here that a clean separation between the two hypotheses has been achieved. The corresponding $K\bar{K}$ effective-mass distributions (not shown) give evidence for strong φ production over negligible backgrounds. The total sample consists of 313 ± 18 φ events in Reactions (7) and (8) and 84 ± 10 φ events in Reaction (9). The

corresponding cross section⁷ for Reaction (1a) is 60 ± 7 (41 ± 4) μb and for Reaction (1b) is 33 ± 7 (20 ± 5) μb at 3.9 (4.6) GeV/ c . The data for Reactions (2a) and (2b) come from a recent π^-p CERN bubble-chamber experiment at 3.9 GeV/ c .⁸

We now compare Reaction (1a) with (2a). The cross section⁹ in the momentum-transfer region¹⁰ $-t' < 1.0$ GeV² for Reaction (1a) is 54 ± 6 μb , to be compared to that for Reaction (2a) which is 64 ± 6 μb . Considering the normalization uncertainties inherent in comparing data from two different experiments, these values are in good agreement with each other. The differential cross sections shown in Fig. 1 are also, bin by bin, in excellent agreement. We have fitted each distribution by the form $d\sigma/dt' \sim e^{At'}$ and obtained¹¹

$$A = 1.9 \pm 0.2 \text{ GeV}^{-2} \text{ for Reaction (1a),}$$

$$A = 2.4 \pm 0.3 \text{ GeV}^{-2} \text{ for Reaction (2a).}$$

The φ density-matrix elements obtained by maximum-likelihood fits, using the P -wave form for the angular distribution in the φ region $1.0 \leq M(K\bar{K}) \leq 1.04$ GeV for the combined 3.9- and 4.6-GeV/ c data¹² (K^+K^- and $K_1^0K_2^0$ events combined) as a function of momentum transfer, are shown in Figs. (2a)–(2f) as open circles in both the Jackson and helicity frames. The corresponding density-matrix elements from Reaction (2a) are shown as closed circles in the figure. We observe remarkably good agreement between the values of $\rho_{mm'}$ as functions of momentum transfer.

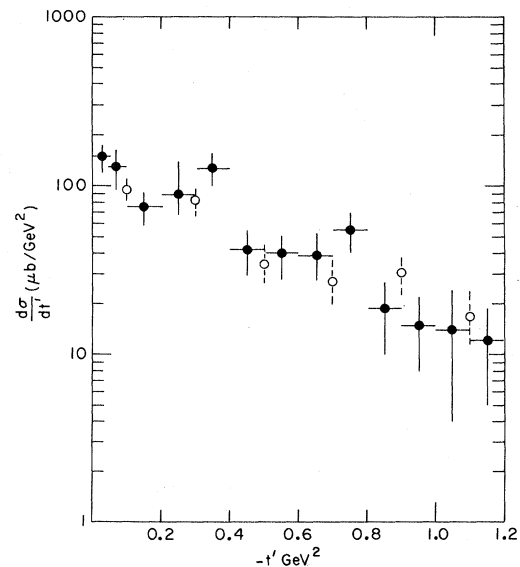


FIG. 1. Differential cross sections for the reactions $K^-p \rightarrow \Lambda\varphi$ (open circles in intervals of 0.2 GeV^2) and $\pi^-p \rightarrow \Lambda K(890)$ (closed circles) at 3.9 GeV/ c .

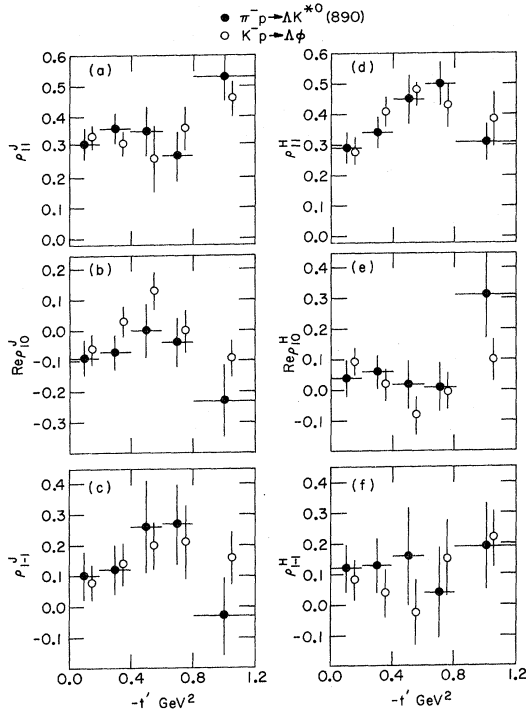


FIG. 2. (a)–(c) Density-matrix elements in the Jackson frame. (d)–(f) Density-matrix elements in the helicity frame. The ϕ and $K(890)$ data are plotted in the same t' intervals.

Finally, in Fig. 3(a) are presented the Λ polarization distributions as functions of momentum transfer for the two reactions. We observe that both reactions exhibit similar polarization in the momentum-transfer region shown. The shapes of these distributions are in marked contrast to those observed in the reactions¹³ $K^-p \rightarrow \Lambda\rho$ and

$K^-p \rightarrow \Lambda\omega$ in our 3.9- and 4.6-GeV/c data, which are shown in Fig. 3(b) for the same momentum-transfer region.

We now perform similar comparisons with the Σ^0 reactions, namely, Reactions (1b) and (2b). The $d\sigma/dt'$ distributions for these reactions are displayed in Fig. 4.¹⁴ They are observed to be in good agreement with the equality suggested from this simple SU(3) approach, as are the corresponding $\rho_{mm'}$ distributions (not shown). The cross section for $-t' < 1.0 \text{ GeV}^2$ is found to be $25 \pm 5 \mu\text{b}$ (includes the relative correction factor to σ of 1.05) for Reaction (1b) compared to $27 \pm 5 \mu\text{b}$ for Reaction (2b) in excellent agreement with each other, as are the fitted values of the slope parameters for the two reactions which were found to be

$$A = 1.1 \pm 0.4 \text{ GeV}^{-2} \text{ for Reaction (1b),}$$

$$A = 1.3 \pm 0.3 \text{ GeV}^{-2} \text{ for Reaction (2b).}$$

On the other hand, these slopes are both about 2 standard deviations smaller than in the corresponding Λ reactions whose values are quoted above.

In summary, we have found that the simple SU(3) relation (3) is in good agreement with the experimentally observed distributions for both Σ^0 and Λ reactions at an incident momentum of 3.9 GeV/c. This justifies, *a posteriori*, that the mass-dependent kinematic factors (e.g., the threshold and pseudothreshold factors) and absorptive effects do not significantly affect the equality (3). It is indeed remarkable to see that further dynamical considerations, such as these, do not lead to a gross violation of a simple SU(3) picture.

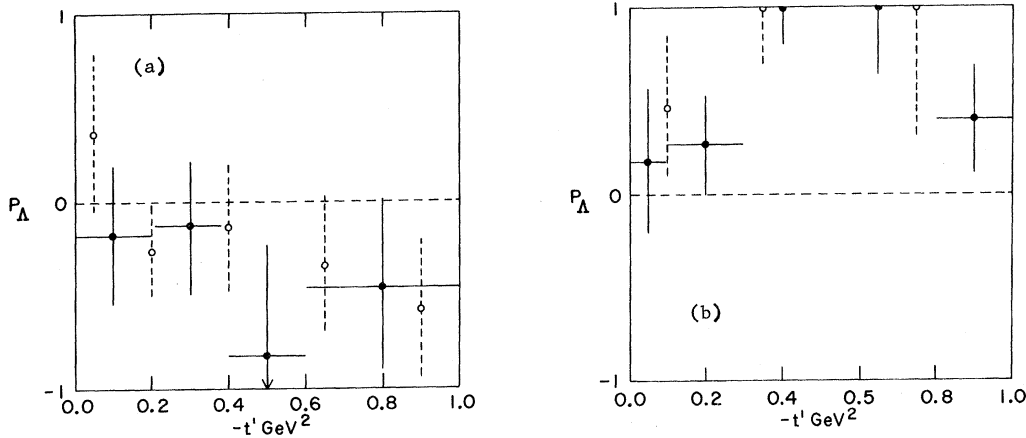


FIG. 3. (a) Λ polarization from the reaction $K^-p \rightarrow \Lambda\phi$ (open circles) and $\pi^-p \rightarrow \Lambda K(890)$ (closed circles). (b) Λ polarization from the reaction $K^-p \rightarrow \Lambda\rho$ (open circles) and $K^-p \rightarrow \Lambda\omega$ (closed circles).

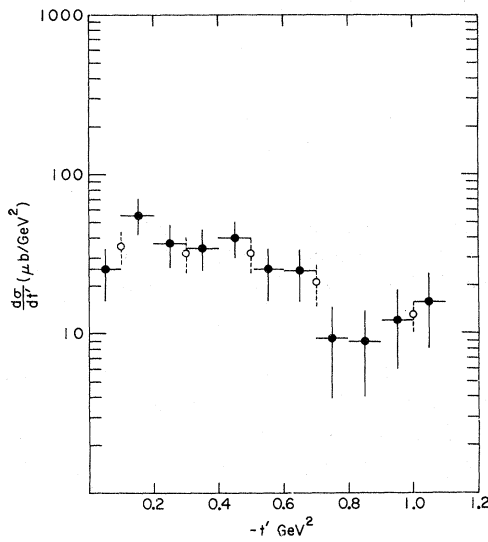


FIG. 4. Differential cross sections for the reactions $K^-p \rightarrow \Sigma^0\phi$ (open circles) and $\pi^-p \rightarrow \Sigma^0K(890)$ (closed circles). The ϕ data are plotted in t' intervals of 0.2 GeV^2 except for the last point whose interval is 0.4 GeV^2 .

We acknowledge many helpful discussions with Dr. R. Field. We thank Dr. M. Abramovich from CERN for sending us the π^-p data before its publication. We also thank the staffs of the alternating-gradient synchrotron and 80-in. bubble chamber for their help in obtaining the pictures, and our data-handling personnel for their efforts.

*Work supported by the U. S. Atomic Energy Commission.

¹See, for instance, the review by G. Fox, in *Phenomenology in Particle Physics, 1971, Proceedings of the Conference at the California Institute of Technology, Pasadena, 25-26 March 1971* (California Institute of Technology, Pasadena, 1971).

²J. Mott, R. Ammar, R. E. P. Davis, W. Kropac, F. Schweingruber, M. Derrick, T. Fields, L. G. Hyman, J. Loken, and J. Simpson, *Phys. Rev. Lett.* **18**, 355 (1967).

³In particular, the following relations are obtained in the peripheral region: F coupling, $-A(K^-p \rightarrow Y\phi)$

$= -6^{-1/2}A_F^8 = A(\pi^-p \rightarrow YK(890))$; D coupling, $-A(K^-p \rightarrow Y\phi) = (\frac{3}{10})^{1/2}A_D^8 = A(\pi^-p \rightarrow YK(890))$; where A_F^8 (A_D^8) is the antisymmetric (symmetric) SU(3) octet amplitude. For more details see H. J. Lipkin, *Nucl. Phys.* **B7**, 321 (1968); G. Alexander, H. J. Lipkin, and F. Scheck, *Phys. Rev. Lett.* **17**, 412 (1966).

⁴S. Meshkov, G. A. Snow, and G. B. Yodh, *Phys. Rev. Lett.* **12**, 87 (1964).

⁵The corresponding events per microbarn after correction for scanning efficiency, film coverage, fiducial volume, and throughput efficiency for Reactions (7) and (9) are 5.1 and 7.4 at 3.9 and 4.6 GeV/c , respectively; for Reaction (8), they are 7.1 and 10.4 at the same two momenta, respectively.

⁶M. Aguilar-Benitez, S. U. Chung, R. L. Eisner, and N. P. Samios, to be published.

⁷The cross sections have been corrected for Λ visibility and losses and for unseen resonance decay modes. They are based on the ϕ branching ratios as determined in our experiment: $(\phi \rightarrow K_1^0 K_2^0)/(\phi \rightarrow K^+ K^-) = 0.89 \pm 0.10$ and $(\phi \rightarrow \pi^+ \pi^- \pi^0)/(\phi \rightarrow K^+ K^-) = 0.28 \pm 0.09$.

⁸M. Abramovich, V. Chaloupka, S. U. Chung, H. G. Hilpert, M. Jacob, M. Korkea-Aho, L. Montanet, S. Reucroft, and J. Zatz, to be published.

⁹The $\Lambda\phi$ cross section has been multiplied by 1.04 to take into account its relative correction to $\bar{\sigma}$ with respect to the $\Lambda K(890)$ cross section. The same factor also multiplies the $d\sigma/dt'$ distribution shown in Fig. 1.

¹⁰We define t' as $t - t_{\text{max}}$, where t is the momentum transfer between the target proton and the outgoing Λ ; $-t_{\text{max}}$ is the minimum momentum transfer for a given event.

¹¹The corresponding slope for Reaction (1a) at 4.6 GeV/c is $2.0 \pm 0.2 \text{ GeV}^{-2}$.

¹²We have found no significant difference in the values of $\rho_{mm'}$ between 3.9 and 4.6 GeV/c . Also, no differences were observed between the $K^+ K^-$ and $K_1^0 K_2^0$ samples.

¹³Simple SU(3) considerations would predict that the observables for $\Lambda\omega$ equal those for $\Lambda\rho$ but both are different from those for $\Lambda\phi$ (see footnote 3). Also, arguments concerning broken duality give a difference between the $\Lambda\phi$ polarization (which has a planar duality diagram) and the $\Lambda\omega$ or $\Lambda\rho$ polarization (which both have nonplanar duality diagrams). See, for example, a discussion by R. D. Field, *Phys. Rev. D* **5**, 86 (1972).

¹⁴Because of the small statistics in the $\Sigma^0\phi$ channel, the data at 3.9 and 4.6 GeV/c have been combined and then normalized to the total cross section at 3.9 GeV/c . The resultant $d\sigma/dt'$ distribution has been multiplied by the relative correction factor between $\Sigma^0\phi$ and $\Sigma^0K(890)$ of 1.05.